Photoproduction of Λ and Σ^{0} hyperons off protons with linearly polarized photons at E_{γ}=1.5–3.0 GeV

S. H. Shiu *et al.* (LEPS Collaboration)

Phys. Rev. C **97**, 015208 — Published 31 January 2018

DOI: 10.1103/PhysRevC.97.015208

Photoproduction of Λ and Σ^0 hyperons off protons with linearly polarized photons at $E_\gamma = 1.5 - 3.0$ GeV

S. H. Shiu,[1,2] H. Kohri,[3,1] W. C. Chang,[1] D. S. Ahn,[4] J. K. Ahn,[5] J. Y. Chen,[6] S. Daté,[7] H. Ejiri,[3] H. Fujimura,[8] M. Fujiwara,[3,9] S. Fukui,[3] W. Gohn,[10] K. Hicks,[11] T. Hotta,[3] S. H. Hwang,[12] K. Imai,[13] T. Ishikawa,[14] K. Joo,[10] Y. Kato,[15] Y. Kon,[3] H. S. Lee,[16] Y. Maeda,[17] T. Mibe,[18] M. Miyabe,[14] K. Mizutani,[19] Y. Morino,[18] N. Muramatsu,[14] T. Nakano,[3] Y. Nakatsugawa,[20] M. Niiyama,[19] H. Noumi,[3] Y. Oh,[21] Y. Ohashi,[7] T. Ohta,[22] M. Oka,[3] J. D. Parker,[23] C. Rangacharyulu,[24] S. Y. Ryu,[3] T. Sawada,[25] H. Shimizu,[14] Y. Sugaya,[3] M. Sumihama,[26] T. Tsunemi,[27] M. Uchida,[28] M. Ungaro,[10] and M. Yosoi[3]

(LEPS Collaboration)

[1]*Institute of Physics, Academia Sinica, Taipei 11529, Taiwan*

[2]*Department of Physics, National Central University, Taoyuan City 32001, Taiwan*

[3]*Research Center for Nuclear Physics, Osaka University, Ibaraki, Osaka 567-0047, Japan*

[4]*RIKEN, The Institute of Physical and Chemical Research, Wako, Saitama 351-0198, Japan*

[5]*Department of Physics, Korea University, Seoul 02841, Republic of Korea*

[6]*Light Source Division, National Synchrotron Radiation Research Center, Hsinchu, 30076, Taiwan*

[7]*Japan Synchrotron Radiation Research Institute, Sayo, Hyogo 679-5143, Japan*

[8]*Wakayama Medical College, Wakayama, 641-8509, Japan*

[9]*National Institutes for Quantum and Radiological Science and Technology, Tokai, Ibaraki 319-1195, Japan*

[10]*Department of Physics, University of Connecticut, Storrs, Connecticut 06269-3046, USA*

[11]*Department of Physics and Astronomy, Ohio University, Athens, Ohio 45701, USA*

[12]*Korea Research Institute of Standards and Science (KRISS), Daejeon 34113, Republic of Korea*

[13]*Advanced Science Research Center, Japan Atomic Energy Agency, Tokai, Ibaraki 319-1195, Japan*

[14]*Research Center for Electron Photon Science, Tohoku University, Sendai, Miyagi 982-0826, Japan*

[15]*Kobayashi-Maskawa Institute, Nagoya University, Nagoya, Aichi 464-8602, Japan*

[16]*Department of Physics and Astronomy, Seoul National University, Seoul 151-742, Republic of Korea*

[17]*Proton Therapy Center, Fukui Prefectural Hospital, Fukui 910-8526, Japan*
[18]*High Energy Accelerator Organization (KEK), Tsukuba, Ibaraki 305-0801, Japan*
[19]*Department of Physics, Kyoto University, Kyoto 606-8502, Japan*
[20]*Institute of High Energy Physics, Chinese Academy of Sciences, Beijing 100049, China*
[21]*Department of Physics, Kyungpook National University, Daegu 702-701, Republic of Korea*
[22]*Department of Radiology, The University of Tokyo Hospital, Tokyo 113-8655, Japan*
[23]*Neutron Science and Technology Center, Comprehensive Research Organization for Science and Society (CROSS), Tokai, Ibaraki 319-1106, Japan*
[24]*Department of Physics and Engineering Physics, University of Saskatchewan, Saskatoon, SK S7N 5E2, Canada*
[25]*Physics Department, University of Michigan, Michigan 48109-1040, USA*
[26]*Department of Education, Gifu University, Gifu 501-1193, Japan*
[27]*Graduate School of Science, Kyoto University, Kyoto 606-8502, Japan*
[28]*Department of Physics, Tokyo Institute of Technology, Tokyo 152-8551, Japan*
(Dated: November 14, 2017)

Abstract

We report the measurement of the $\gamma p \to K^+\Lambda$ and $\gamma p \to K^+\Sigma^0$ at SPring-8. The differential cross sections and photon-beam asymmetries are measured at forward K^+ production angles using linearly-polarized tagged-photon beams in the range of $E_\gamma = 1.5-3.0$ GeV. With increasing photon energy, the cross sections for both the $\gamma p \to K^+\Lambda$ and $\gamma p \to K^+\Sigma^0$ reactions decrease slowly. Distinct narrow structures in the production cross section have not been found at $E_\gamma = 1.5 - 3.0$ GeV. The forward peaking in the angular distributions of cross sections, a characteristic feature of t-channel exchange, is observed for the production of Λ in the whole observed energy range. A lack of similar feature for Σ^0 production reflects a less dominant role of t-channel contribution in this channel. The photon-beam asymmetries remain positive for both reactions, suggesting the dominance of K^* exchange in the t-channel. These asymmetries increase gradually with the photon energy, and have a maximum value of +0.6 for both the reactions. Comparison with theoretical predictions based on the Regge-trajectory in the t-channel and the contributions of nucleon resonances indicates the major role of t-channel contributions as well as non-negligible effects of nucleon resonances to account for the reaction mechanism of hyperon photoproduction in this photon energy regime.

PACS numbers: 13.60.Le, 13.60.Rj, 13.88.+e, 14.20.Jn, 25.20.Lj

I. INTRODUCTION

A quantitative understanding of hadronic interactions at low energies has been a long-time challenge. There exist serious difficulties to derive hadronic interactions from the first-principle Quantum-Chromo-Dynamics (QCD) because of its intrinsic non-perturbative property in the low-energy regime. Instead, an alternative approach is the usage of effective theory where the effective Lagrangian is constructed as a sum of all tree-level Feynman diagrams in the s-, t- and u-channel exchanges of possible hadrons in their ground and excited states. Through the comparison of the predictions with the experimental results of the differential production cross sections and polarization observables over a wide-range hadronic reactions using a variety of beams and targets, the hadronic degrees of freedom involved are explored. Recent progress is summarized in Ref. [1, 2]. Nevertheless, the identified baryon resonances in the experiments and lattice QCD calculations [3] are significantly fewer than what have been predicted by the constituent quark model. More experimental and theoretical effort is required to shed light on this "missing" resonance problem [4].

The processes of hyperon (Y) photoproduction has been studied for exploring the nucleon resonances which couple more strongly to KY than to πN. Furthermore, the isospin structure of KY final states filters out some possible intermediate states of nucleon resonances. For example, because of the different isospin (I) properties of Λ ($I = 0$) and Σ^0 ($I = 1$), only $I = 1/2$ N^* intermediate states could couple to $K^+\Lambda$ while both $I = 1/2$ N^* and $I = 3/2$ Δ^* intermediate states are allowed for $K^+\Sigma^0$ production.

At $E_\gamma > 2$ GeV, above the resonance region, the t-channel exchange of strange mesons like K, K^* and K_1 is expected to play an important role at forward angles. The coupling strength of the exchanged strange mesons with the ground-state nucleon can be determined from their t-channel contributions. Measurements of the photon-beam asymmetry help to further define the hadron photoproduction mechanism because of the extreme sensitivity to the model parameters and the presence of resonances. For example, the measurements of the photon-beam asymmetries provide unique information to constrain the possible t-channel exchanges. A photon-beam asymmetry close to -1 is expected for the case of dominating unnatural parity exchange of K or K_1 whereas the dominance of natural parity K^* exchange leads to a photon-beam asymmetry of $+1$.

For the photoproduction of ground-state hyperons Λ and Σ^0 off protons, the measurements of differential cross sections and various polarization observables of $\gamma p \to K^+\Lambda$ and $K^+\Sigma^0$ from threshold up to the photon beam energy $E_\gamma = 16$ GeV have been done by SLAC [5, 6], SAPHIR [7,

8], LEPS [9–11, 18], CLAS [12–14], GRAAL [15, 16] and Crystal Ball [17] experiments. A clear resonance structure in the production cross sections around a center of mass energy $\sqrt{s} = 1.9 - 1.96$ GeV was observed in the $K^+\Lambda$ channel [7, 8, 10, 12, 13], and small enhancement was found at $\sqrt{s} = 2.05$ GeV at forward angles in the $K^+\Sigma^0$ channel [7, 8, 10, 12, 14]. The photon-beam asymmetries both for the two channels were seen to be positive, and that of $K^+\Sigma^0$ production was in general the larger of the two. In addition, similar reaction channels for $\gamma n \to K^+\Sigma^-$ and $\gamma p \to K^0\Sigma^+$ have also been identified experimentally [18–24].

Several theoretical analyses have been performed. A common approach is the single-or coupled-channel isobar models, e.g. Kaon-MAID (KAMID) [25–28]. In general, there are a great amount of parameters required in modeling of all possible s-, t- and u-channel Feynman diagrams. This introduces difficulties in determining such parameters reliably from a limited number of data points available.

On the other hand, Regge theory is well known, with an elegant formalism in modeling high-spin and high-mass particle exchange at large s and small $|t|$ or $|u|$. It is very successful in describing the diffractive production at high energies. The applicability of Regge theory in the low-energy regime is, however, controversial. Recently, people started to adopt Regge theory for modeling the t-channel contribution in an effective theory by replacing the usual pole-like Feynman propagator with a corresponding Regge propagator. The number of free parameters was significantly reduced. In Ref. [29], it was found that the photoproduction of Λ and Σ^0 for $E_\gamma = 5 - 16$ GeV could be well described by a modified t-channel exchange of K and K^* Regge trajectories, together with a corresponding modification of the s-channel nucleon pole contribution. Later, the same approach was successfully extended to describe the data in the energy region down to $E_\gamma = 2$ GeV [30]. Therefore, it becomes a popular approach to use K and K^* Regge trajectories in modeling the t-channel contributions in hyperon photoproduction.

In the Bonn-Gatchina (BG) model [31–35], the strength of Regge theory t-channel terms are determined simultaneously with the resonance contributions in s-channels through the data fitting. In contrast, the Regge-plus-resonance (RPR) model [36–38] treats the t-channel as a background and fixes its contribution in advance by high-energy data at forward production angles [37, 38], where a forward-peaking behavior in the angular distributions is clearly observed. The resonance contributions in s-channels are then added for extrapolation to the resonance regions. Through these studies, the evidence of a number of nucleon resonances contributing to hyperon photoproduction has been reported [27, 33, 38, 39], e.g. $S_{11}(1650)$, $P_{11}(1710)$, $P_{13}(1720)$ and $D_{13}(1900)$

for N^*, and $S_{31}(1900)$, $P_{31}(1910)$, $D_{33}(1700)$ and $P_{33}(1920)$ for Δ^*.

In the present work, we report on the measurement of the differential cross sections and photon-beam asymmetries in the energy region of $E_\gamma = 1.5 - 3.0$ GeV at very forward angles. The new results fill the gap at $E_\gamma = 2.5 - 6.0$ GeV in the existing measurements, providing a strong constraint in modeling Regge trajectories in the t-channel at lower energies, and helping to pin down the contributions of heavier nucleon resonances in the transition region. The present paper is outlined as follows. In Sec. II, the experimental setup and the analysis methods are introduced. The results and a comparison with the theoretical predictions is presented in Sec. III. A summary is given in Sec. IV.

II. EXPERIMENT AND DATA ANALYSIS

The experiment was carried out in the Laser-Electron-Photon beamline (LEPS) at the SPring-8 facility in Japan. The photon beam was generated by the laser backscattering technique using a deep-UV laser with a wavelength of 257 nm [40]. The energy range of the tagged photon beams is 1.5-3.0 GeV, corresponding to $\sqrt{s} = 1.92 - 2.53$ GeV. The degree of linear polarization for the tagged photon beams is 88% at $E_\gamma = 3.0$ GeV, and drops down to 28% at $E_\gamma = 1.5$ GeV.

The photon beam was incident on a liquid hydrogen target with an effective length of 16 cm. Charged particles produced at the target were detected by the LEPS spectrometer in the very forward direction; the angular coverage is about ± 0.4 and ± 0.2 rad in the horizontal and vertical directions, respectively. The spectrometer consisted of a dipole magnet, a silicon vertex detector and three drift chambers. A time of flight (TOF) measurement for charged particles was done using a start counter (SC) scintillator 5 cm downstream of the target together with TOF wall, an array of scintillator bars placed 4 m downstream of the target. At the end of the beam pipe, an upstream veto (UPveto) counter made by plastic scintillator to eliminate the e^+e^- background events has been installed. The event trigger was a coincidence of the tagger, UPveto, the SC and the TOF wall. Since the data set was originally collected for detecting K^{*0} decaying to high-momentum K^+ and π^- [41], the regular spectrometer setup was slightly modified. We removed the Aerogel Cherenkov counter, which had been placed immediately after the target in earlier experiment to reject high-momentum electrons, positrons, and pions at the trigger level. The signal from a plastic scintillation counter placed downstream of the drift chambers was used to veto e^+e^- pairs produced from photon conversion. For further details concerning the detector configuration and

the quality of particle identification, refer to Ref. [10, 42].

Particle identification (PID) of the charged particles was done by a 3σ cut on their reconstructed masses based on the measured TOF, momentum and path length, where σ is the momentum dependent mass resolution. Pions and kaons were well separated in the momenta region lower than 1.0 GeV/c. To ensure good PID by removing K^+ decay-in-flight, an extrapolation of the hit position (using the Runge Kutta method) from the drift chamber to the TOF wall was applied. We required the extrapolated vertical hit position to be within 8 cm of the estimated one based on the time difference of TOF readout from both ends of the fired scintillator bar. For the horizontal hit position, the difference of channel number of the extrapolated TOF slat and the fired one was required to be less than 2.

With the cuts of an identified K^+ within 3σ mass resolution, a minimum mass of 0.4 GeV/c^2, and a vertex position on the liquid hydrogen target, the missing mass spectrum for the reaction $\gamma p \to K^+X$ ($\mathrm{MM}_X(\gamma p, K^+)$) is shown in Fig. 1 where the $K^+\Lambda$ and $K^+\Sigma^0$ events are clearly observed as well as the production of higher hyperon resonances such as $\Sigma^0(1385)/\Lambda(1405)$ and $\Lambda(1520)$. The numbers of $K^+\Lambda$ and $K^+\Sigma^0$ events are about 2.6×10^4 and 1.8×10^4, respectively.

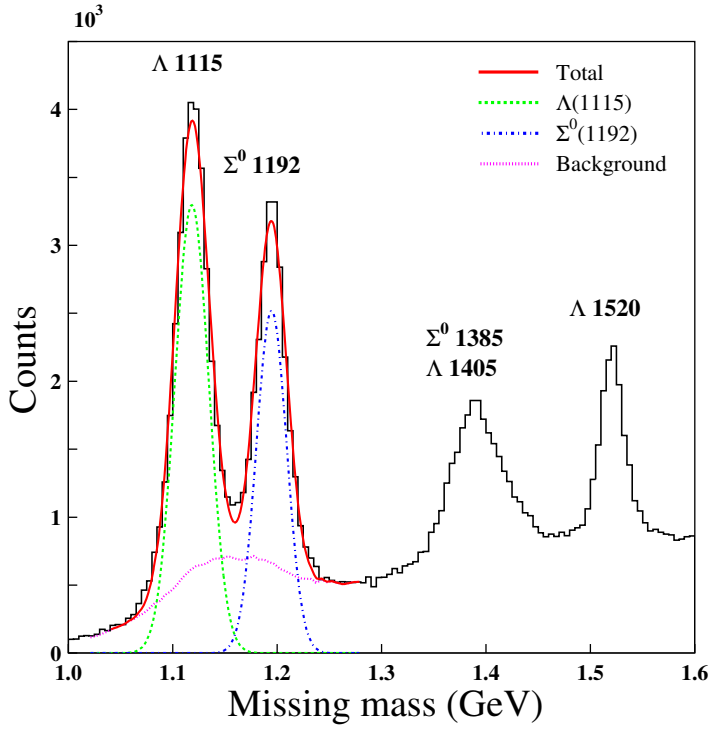

FIG. 1. Missing mass spectrum of $\gamma p \to K^+X$ reaction ($\mathrm{MM}_X(\gamma p, K^+)$) at $E_\gamma = 1.5 - 3.0$ GeV.

Compared to the previous LEPS experiment [10], the background level under the Λ and Σ^0

peaks in the missing mass spectrum $\mathrm{MM}_X(\gamma p, K^+)$ was enhanced in the current study. This is due to the removal of Aerogel Cherenkov counter as mentioned above, and there happened to be contamination of pions in the selected K^+ with momentum higher than 1.0 GeV/c. The degree of pion contamination in the selected kaons increased for particles of larger momenta. Therefore, the fraction of background in the missing mass spectra was enhanced at larger E_γ and at smaller kaon production angles.

We used a side-band subtraction for eliminating background events caused by the misidentified π^+. A side-band sample was chosen by using π^+ events lying outside of the K^+ mass region in the same bin of track momentum ($|\vec{P}|$), photon energy (E_γ), and production angle ($\cos\theta^{K^+}_{c.m.}$). Using the momentum information of π^+ particles in side-band sample, the background template in $\mathrm{MM}_X(\gamma p, K^+)$ was constructed by assuming the kaon mass for the pion tracks. With this background template, Monte-Carlo simulated the $\mathrm{MM}_X(\gamma p, K^+)$ for Λ and Σ^0 production in the same $\{|\vec{P}|, E_\gamma, \cos\theta^{K^+}_{c.m.}\}$ bin. A normalization of the background template was obtained by fitting the experimental $\mathrm{MM}_X(\gamma p, K^+)$ data in the mass range of 1.0-1.26 GeV/c^2. The corresponding ranges of $|\vec{P}|$, E_γ, and $\cos\theta^{K^+}_{c.m.}$ kinematic variables are 0-3 GeV/c, 1.5-3.0 GeV and 0.6-1.0, respectively. After fixing the normalization in each bin, we summed up the background template over all the track momentum ($|\vec{P}|$) bins to obtain the combined background template in each $\{E_\gamma$, $\cos\theta^{K^+}_{c.m.}\}$ bin. The yields of the $K^+\Lambda$ and $K^+\Sigma^0$ production were extracted using another new fit of the missing mass spectrum, with two Gaussian distributions having constant peaks at standard PDG masses and free widths for the signals, and the combined background template.

Figure 1 shows that the missing mass spectrum around the signal region of the $K^+\Lambda$ and $K^+\Sigma^0$ events is well described using two Gaussian distributions of signal (green dotted line for $K^+\Lambda$ and blue one for $K^+\Sigma^0$) and a background template from the side-band of the kaon mass regions (purple dotted line). The broad bump structure in the background under the Λ and Σ^0 peaks is caused by the mis-identification of π^+ in the $\gamma p \to \pi^+\Delta^0$ reaction. Another possible background source is the photoproduction of ϕ mesons and their charged kaon decays. The missing mass distribution of ϕ production is expected to appear above 1.5 GeV/c^2 in Fig. 1. Therefore it does not constitute a background in the signal region of interest for the Λ and Σ^0 productions.

In each kinematic bin of E_γ and $\cos\theta^{K^+}_{c.m.}$, the cross sections for $K^+\Lambda$ and $K^+\Sigma^0$ photoproduction were evaluated using the measured yields, the integrated photon flux from the tagger, the liquid target density, correction factors for the K^+ detection and the photon tagging inefficiencies. The K^+ detection efficiency was estimated based on Monte-Carlo simulations by assuming a uni-

form production of $K^+\Lambda$ and $K^+\Sigma^0$ in E_γ and $\cos\theta^{K^+}_{c.m.}$. The acceptance of the LEPS spectrometer was simulated using the GEANT software. The simulated peak widths for the missing mass of K^+ on Λ and Σ^0 were in good agreement with those shown in Fig. 1.

The systematic uncertainty was estimated by a variation of the background template. Since there were impurities of e^+ and K^+ particles in the selected π^+ region used for the background template, we observed a dependence of the background template on different choices of the selected π^+ region as well as the momentum binning. The variation range of results, corresponding to the changes on the above two factors, was assigned as the major systematic uncertainty. There were additional systematic uncertainties due to the photon beam flux and the target length which were estimated to be 3% and 1%, respectively.

Using both event yields with the vertically (V) and horizontally (H) polarized photon beams, the photon-beam asymmetry (Σ_γ) of $K^+\Lambda$ and $K^+\Sigma^0$ photoproduction is given as follows:

$$P_\gamma \Sigma_\gamma \cos(2\phi_{K^+}) = \frac{nN_{\rm V} - N_{\rm H}}{nN_{\rm V} + N_{\rm H}} \tag{1}$$

where P_γ stands for the polarization degree of the photon beams and ϕ_{K^+} denotes the azimuthal production angle of detected K^+ with respect to the horizontal plane in the lab system. The $N_{\rm V}$ and $N_{\rm H}$ are the individual hyperon production yields from the vertically and horizontally polarized photon beams, and n is the normalization factor defined by the photon flux ratio of two polarization directions ($n = n^\gamma_{\rm H}/n^\gamma_{\rm V}$), which is 1.014 for this study. Figure 2 shows the ratio $(nN_{\rm V} - N_{\rm H})/(nN_{\rm V} + N_{\rm H})$ as a function of ϕ_{K^+} for the $K^+\Lambda$ and $K^+\Sigma^0$ channels at $E_\gamma = 2.7$ GeV and $\cos\theta^{K^+}_{c.m.} = 0.9$. The ratios are largest at ϕ_{K^+} = 0°, 180° and 360°, and smallest at ϕ_{K^+} = 90° and 270° for both the channels. This means that K^+ mesons prefer to scatter at ϕ_{K^+} angles perpendicular to the polarization plane, suggesting positive photon-beam asymmetries. The lines overlaid are the best fit of a $\cos(2\phi_{K^+})$ modulation.

III. RESULTS

A. Differential cross sections

The differential cross sections for the $K^+\Lambda$ and $K^+\Sigma^0$ reactions as a function of photon beam energy E_γ in the range of $0.6 < \cos\theta^{K^+}_{c.m.} < 1.0$ are shown in Fig. 3. The error bars represent the statistical errors while the hatched area expresses the range of systematic uncertainty. The theoretical predictions from the RPR model [43] with (RPR, solid red lines) and without resonances

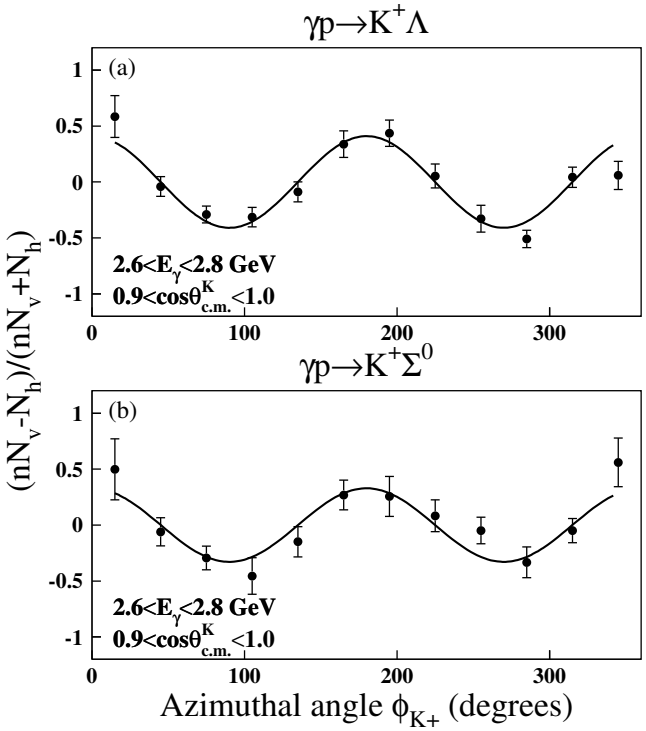

FIG. 2. Azimuthal angle (ϕ_{K^+}) dependence of the ratio $(nN_{\rm V} - N_{\rm H})/(nN_{\rm V} + N_{\rm H})$ in Eq. 1 for the (a) $K^+\Lambda$ and (b) $K^+\Sigma^0$ channels at $E_\gamma = 2.7$ GeV and $\cos\theta^{K^+}_{c.m.} = 0.9$. The solid lines are the fit results using a function of $\cos 2\phi_{K^+}$.

(RPR-Regge, dashed blue lines) as well as BG2014-02 solutions [44] of Bonn-Gatchina (BG) models (dot-dashed green lines) are overlaid for comparison. We use RPR-2011 solutions [38] for $K^+\Lambda$ and RPR-2007 ones [37] for $K^+\Sigma^0$.

Within $E_\gamma = 1.5 - 3.0$ GeV, the differential cross sections for the $K^+\Lambda$ channel decrease monotonically with the beam energy in all four bins of $0.6 < \cos\theta^{K^+}_{c.m.} < 1.0$. No distinct narrow resonance structure is observed. In contrast, the previous LEPS analysis [10] suggests the observation of a small bump structure around $E_\gamma = 1.5 - 1.6$ GeV ($\sqrt{s} = 1.92 - 1.97$ GeV). In this analysis, the larger photon energy bin size prevents us from identifying the structure. The cross sections for the $K^+\Lambda$ channel are larger than those for the $K^+\Sigma^0$ channel. The cross sections for the $K^+\Sigma^0$ channel also shows a decreasing trend with the beam energy whereas its energy dependence is relatively mild compared to the $K^+\Lambda$ channel. The mild energy dependence for the $K^+\Sigma^0$ channel is consistent with non-negligible s-channel contributions. Although there is no distinct narrow resonance structure in the $K^+\Sigma^0$ cross sections, some resonance, like structures are seen at E_γ ~1.8 GeV and 2.8 GeV ($\sqrt{s}$ ~2.06 GeV and 2.47 GeV) at $0.7 < \cos\theta^{K^+}_{c.m.} < 1.0$.

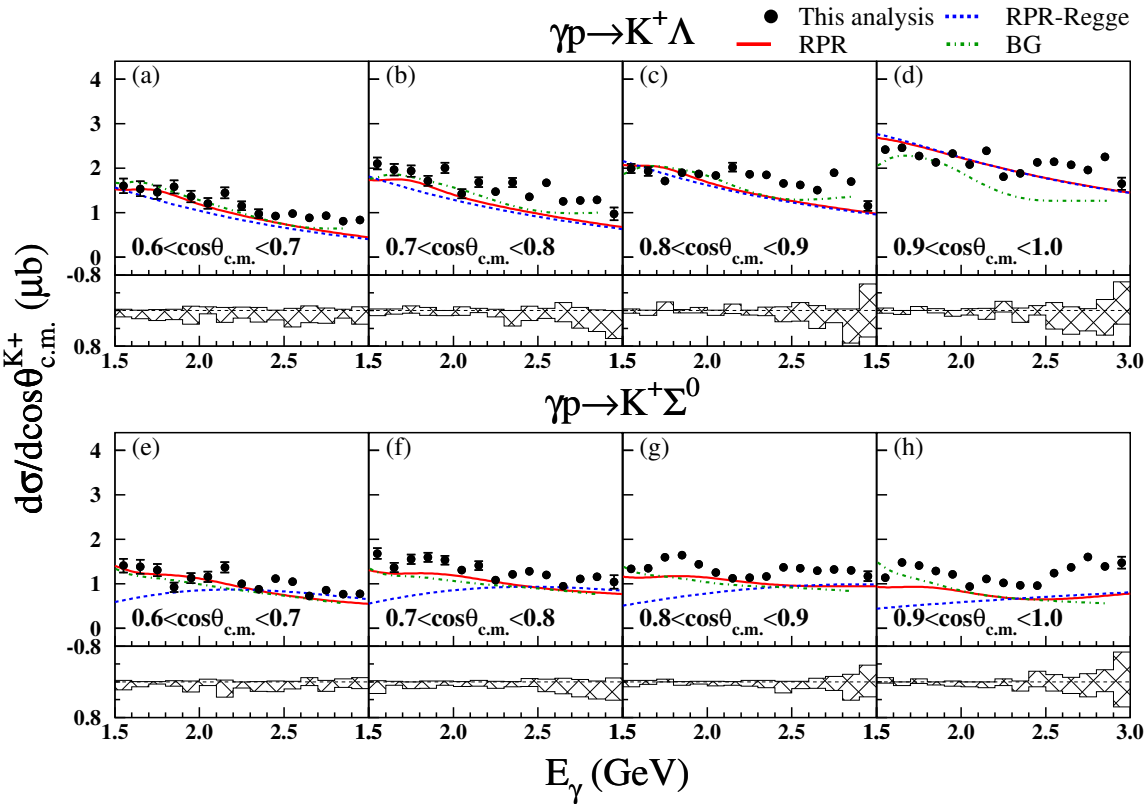

FIG. 3. Differential cross sections for the $p(\gamma,K^+)\Lambda$ reaction (a)$\sim$(d) and for $p(\gamma,K^+)\Sigma^0$ reaction (e)$\sim$(h) as a function of photon energy E_γ for the kaon C.M. production polar angle $0.6 < \cos\theta^{K^+}_{c.m.} < 1.0$. The curves denote the predictions of Regge-model [43] calculation with (RPR, solid red lines) and without resonances (RPR-Regge, dashed blue lines), and Bonn-Gatchina model (BG, dot-dashed green lines). The hatched histograms indicate the systematic uncertainty.

These structures have also been observed by CLAS at $\cos\theta^{K^+}_{c.m.} = 0.9$ [12, 14].

In comparing the real data with theoretical predictions, both RPR(-Regge) and BG models fail to give a good description of the data of $K^+\Lambda$ and $K^+\Sigma^0$ except for the most backward bin of $\cos\theta^{K^+}_{c.m.} = 0.65$. The current new results shall enable an improvement of theoretical modeling at the forward direction for both $K^+\Lambda$ and $K^+\Sigma^0$ channels. The structures observed at $E_\gamma \sim 1.8$ GeV and 2.8 GeV ($\sqrt{s} \sim 2.06$ GeV and 2.47 GeV) over $0.7 < \cos\theta^{K^+}_{c.m.} < 1.0$ in $K^+\Sigma^0$ channel can not be well reproduced by both theoretical predication. The difference between the predictions of RPR (red solid lines) and RPR-Regge (blue dashed lines) indicates the contributions of nucleon resonances in the s-channel in $K^+\Sigma^0$ production at $E_\gamma < 2.2$ GeV.

In Figs. 4 and 5, the same data are drawn as a function of the reduced four-momentum transfer

$|t - t_{min}|$, for fifteen photon energy bins within $E_\gamma = 1.5 - 3.0$ GeV, where t_{min} denotes t at zero degrees. Other than the theoretical predictions of RPR and BG, the previous results of LEPS 2006 [10] (red open squares), SAPHIR 2004 [8] (yellow open cross), CLAS 2006 [12] (blue open triangles), and CLAS 2010 [13, 14] (purple open triangles) are displayed as well. Considering the overall errors, the current results agree with previous measurements in overlapping kinematic regions. For two sets of CLAS data [12–14], CLAS 2010 agree better with our results in $K^+\Lambda$ channel while a better agreement with CLAS 2006 in $K^+\Sigma^0$ channel.

There are qualitative differences in the t-dependence of the differential cross sections for $K^+\Lambda$ and $K^+\Sigma^0$ at forward angles. At low energies, the production of $K^+\Lambda$ shows a clear increase toward $t = t_{min}$. Above $E_\gamma > 2.2$ GeV, the presence of a plateau with a close-to-zero slope near $t = t_{min}$ is observed for the $K^+\Lambda$ channel. This observation is consistent with the measurements at $E_\gamma = 5$ GeV [5]. There even appeared a decrease of the cross sections toward $t = t_{min}$ for $E_\gamma = 8$, 11 and 16 GeV [5]. As for the $K^+\Sigma^0$ production, the overall t-dependence is roughly flat for $E_\gamma < 1.7$ GeV. A plateau structure near $t = t_{min}$ with a finite negative slope beyond $|t - t_{min}| < 0.3$ GeV^2 appears in $E_\gamma = 1.7 - 2.7$ GeV. Going beyond $E_\gamma > 2.7$ GeV, the t-dependence of the differential cross sections nears a monotonic increase toward $t = t_{min}$.

In Ref. [29], the main contributions to $K^+\Lambda$ production for $E_\gamma > 5$ GeV are described by the reggeized K^*-exchange in t channel and the differential cross sections have an exponential t-dependence but decrease quickly to zero at $t = t_{min}$. The plateau near $t = t_{min}$ in the differential cross sections at $E_\gamma = 5$ GeV was interpreted as due to the contributions of a reggeized s-channel diagram, which is necessitated by gauge invariance and required only for K-exchange. Beyond the very forward region at $|t - t_{min}| \approx m_K^2$, i.e. 0.25 GeV^2, K^*-exchange gives the main contribution to the cross sections. The lack of a similar plateau feature in $K^+\Sigma^0$ production is because of a relatively minor contribution of K-exchange arising from a weak coupling among K, Σ^0 and nucleons [29].

The model of contributions of a reggeized s-channel diagram for K-exchange at the region of $|t - t_{min}| \approx m_K^2$ provides a reasonable qualitative description of what we observe in hyperon production at $E_\gamma = 1.5 - 3.0$ GeV. In $K^+\Lambda$ production, we see the same plateau in the t-dependence of the differential cross sections for $E_\gamma > 2.2$ GeV. As the energy decreases, the contributions of K-exchange, characterized by an increase of cross section toward $t = t_{min}$, become more important [10]. In the framework of a Regge model, the energy dependence of the differential cross sections at $t = t_{min}$ scales as $s^{2\alpha_0 - 2}$ where α_0 is the intercept of the Regge trajectory at $t = 0$ [29].

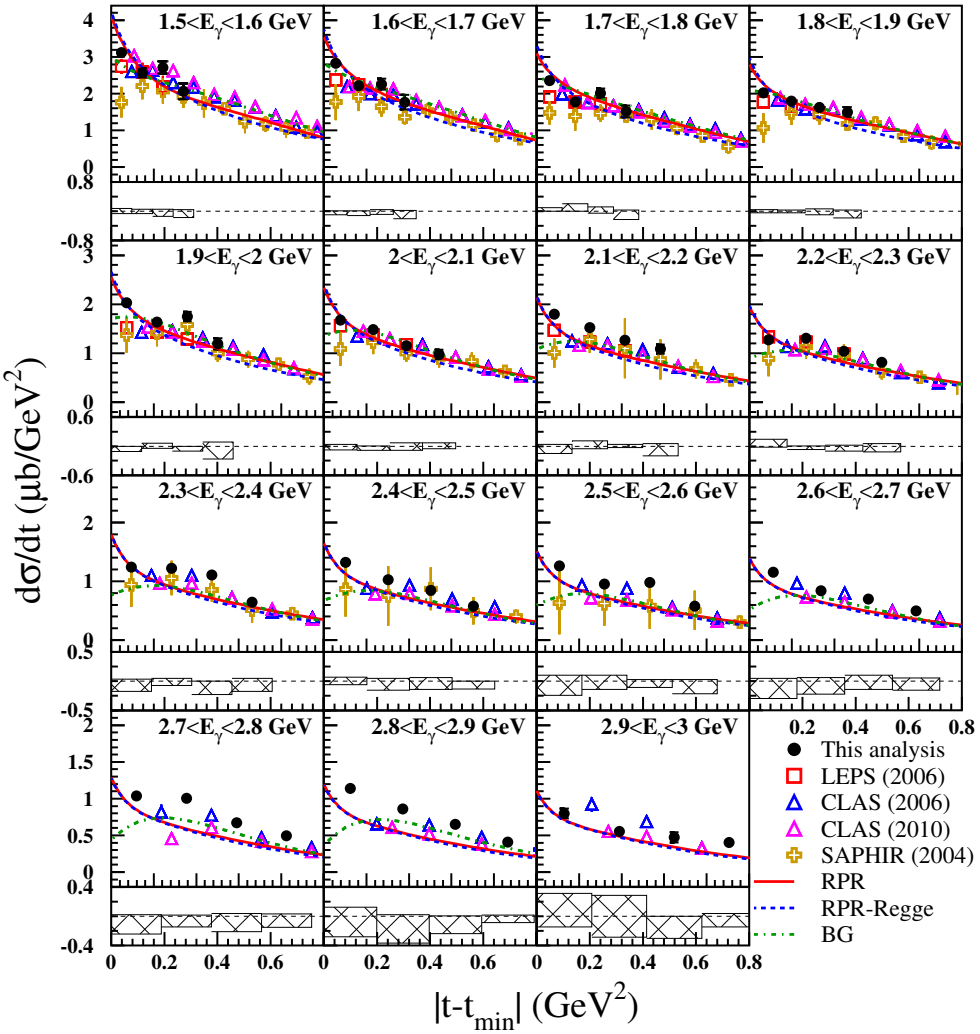

FIG. 4. Differential cross sections for the $p(\gamma,K^+)\Lambda$ reaction as a function of $|t-t_{min}|$ for $1.5 < E_\gamma < 3.0$ GeV. The results of this measurement are shown by solid black circles. The results of LEPS 2006 [10] (red open squares), CLAS 2006 [12] (blue open triangles), CLAS 2010 [13] (purple open triangles), and SAPHIR 2004 [8] (yellow open cross) are also shown. The notations of curves are the same as those in Fig. 3. The shaded histograms show the systematic uncertainty.

The smallness of α_0 of K Regge trajectory, compared with that of K^*, would lead to an increasingly strong contribution from the t-channel K-exchange toward low energies. This expectation indeed agrees with what is observed.

For $K^+\Sigma^0$ production, the contributions of K exchange are negligible overall and thus we do not observe a similar rise toward $t = t_{min}$ at low energies. Instead, the relatively flat t-dependence

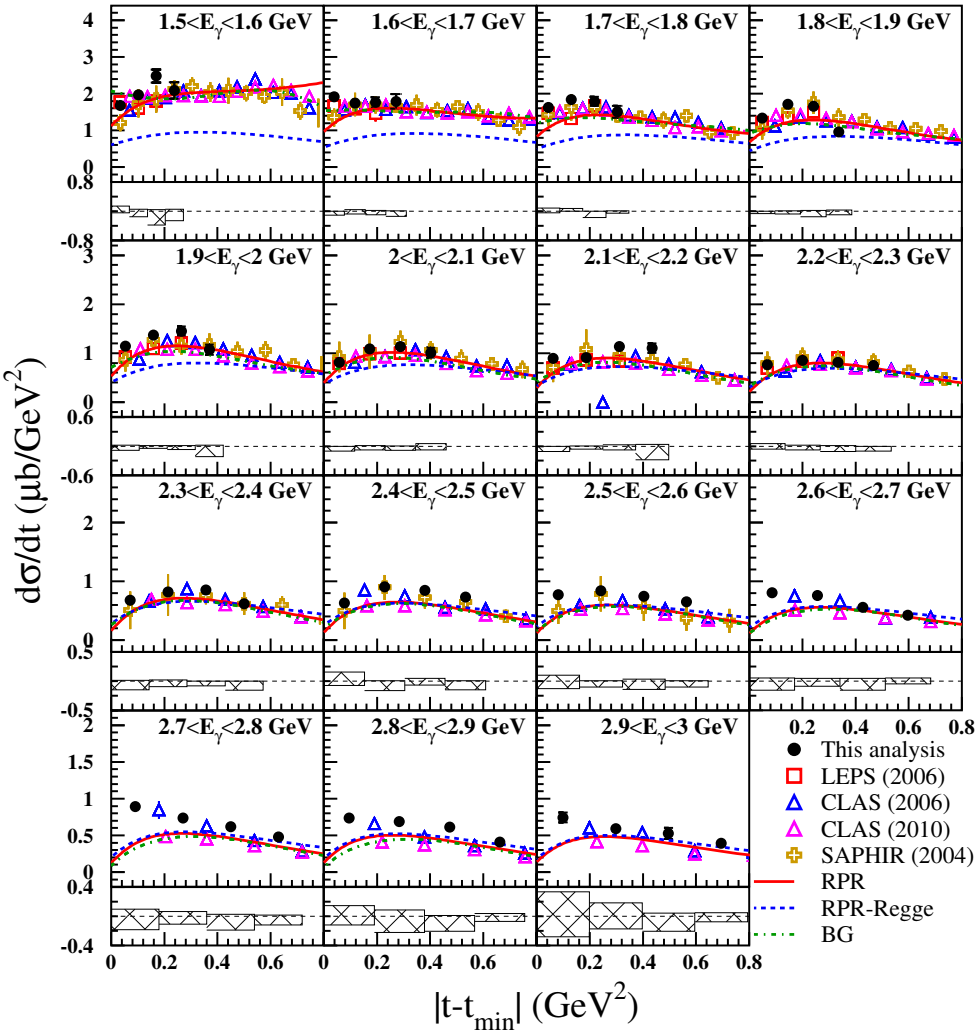

FIG. 5. Differential cross sections for the $p(\gamma,K^+)\Sigma^0$ reaction as a function of $|t-t_{min}|$ for $1.5 < E_\gamma < 3.0$ GeV. The notations of points and curves are the same as those in Fig. 4. The shaded histograms show the systematic uncertainty.

reflects the importance of s-channel nucleon resonance contributions in this channel. This can be understood because only the intermediate nucleon resonances with isospin $I = 1/2$ are allowed for $K^+\Lambda$ production, while both $I = 1/2$ and $3/2$ resonances could work for the case of $K^+\Sigma^0$.

As for a comparison with theoretical models in the $K^+\Lambda$ channel, the RPR model describes the forward-peaking rather well, except that there exists some quantitative deviation from the data for $E_\gamma > 2.1$ GeV. In the region of $|t - t_{min}| > 0.2$ GeV^2, the BG model describes the data slightly better than RPR. But the predictions of the BG model fails to reproduce the increase at the most

forward angle bin for higher energies.

In the $K^+\Sigma^0$ channel, the contribution of resonances is important for $E_\gamma < 2.2$ GeV as seen from the difference between the predictions of RPR and RPR-Regge models. Both RPR and BG models fail to describe the appearance of forward-peaking in the region of $|t - t_{min}| < 0.3$ GeV^2 for $E_\gamma > 2.7$ GeV. This brings up the need of improving the description of Regge trajectories for t-channel contributions in this energy regime.

B. Photon-beam asymmetry

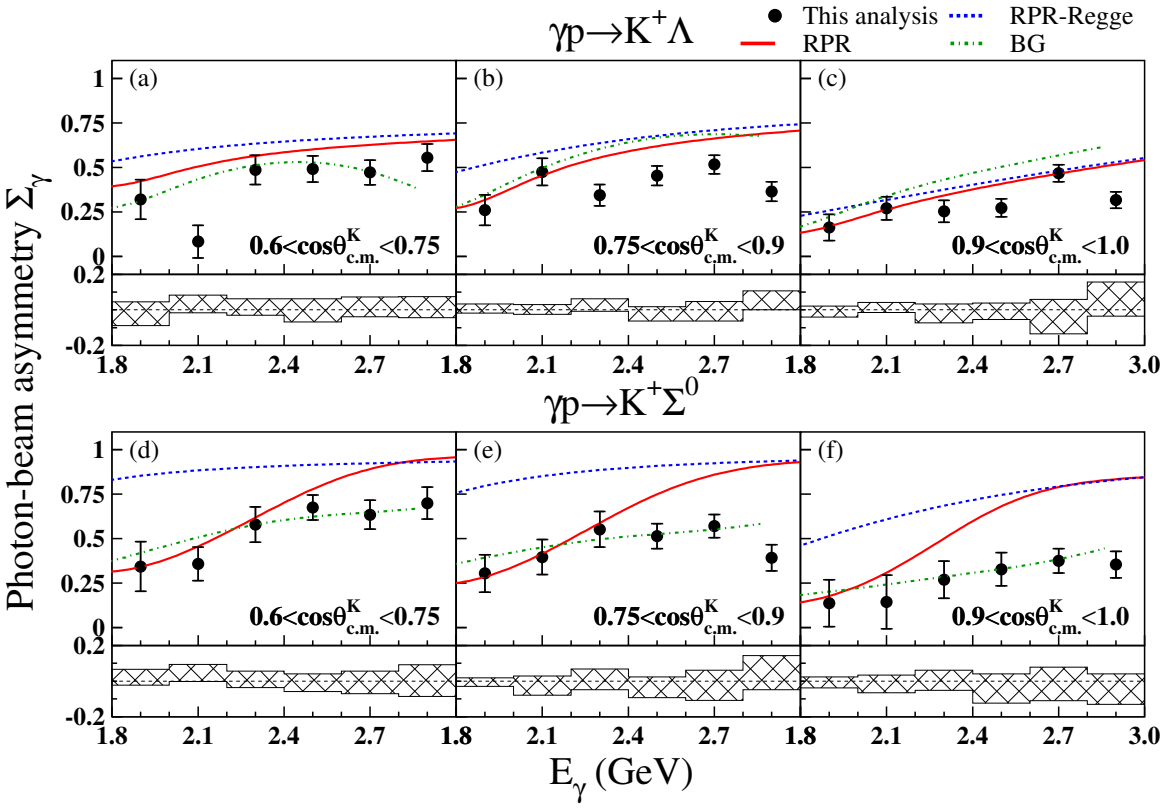

FIG. 6. Photon-beam asymmetries (Σ_γ) for the $p(\gamma,K^+)\Lambda$ reaction (a)$\sim$(c) and for $p(\gamma,K^+)\Sigma^0$ reaction (d)$\sim$(f) with systematic uncertainty plotted in hatched histogram as a function of photon energy E_γ for the kaon C.M. production polar angle $0.6 < \cos\theta^{K^+}_{c.m.} < 1.0$. The notations of curves are the same as those in Fig. 3.

Figure 6 shows the photon-beam asymmetries for the $K^+\Lambda$ and $K^+\Sigma^0$ channels as a function of E_γ for $E_\gamma > 1.8$ GeV in three bins of production angle $0.6 < \cos\theta^{K^+}_{c.m.} < 1.0$. Results at very

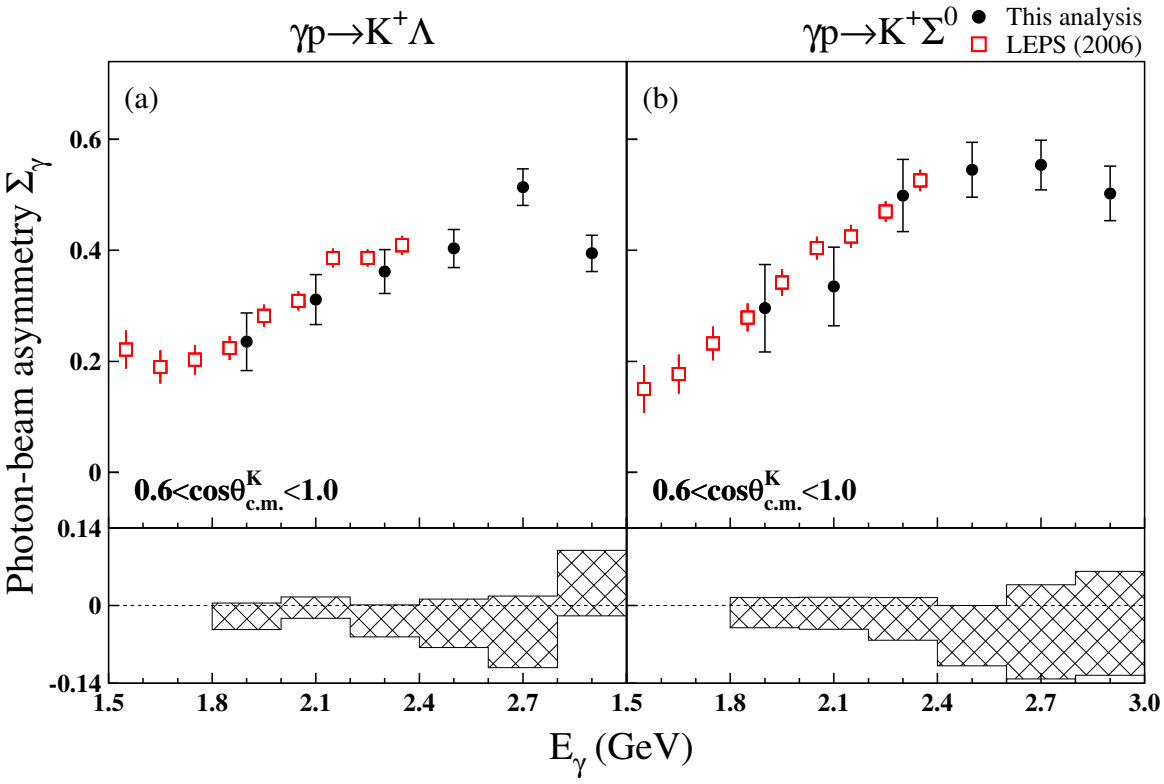

FIG. 7. Photon-beam asymmetries (Σ_γ) for the $p(\gamma,K^+)\Lambda$ reaction (a) and $p(\gamma,K^+)\Sigma^0$ reaction (b) with systematic uncertainty plotted in hatched histogram as a function of E_γ for $0.6 < \cos\theta^{K^+}_{c.m.} < 1.0$. The results of this measurement and, LEPS 2006 are shown by solid black circles and red open squares.

forward angles for photon energies of 2.4-3.0 GeV are obtained for the first time. The photon-beam asymmetries are all positive and show a mild increase with beam energy, from ∼0.1-0.2 at $E_\gamma = 1.9$ GeV to ∼0.5-0.6 at $E_\gamma = 2.9$ GeV. In both channels, a saturation of the photon-beam asymmetries at $E_\gamma = 2.9$ GeV in the production angle $0.75 < \cos\theta^{K^+}_{c.m.} < 1.0$ is observed. In Fig. 7, we plot the photon-beam asymmetries in the whole region of $0.6 < \cos\theta^{K^+}_{c.m.} < 1.0$ together with previous results at slightly lower energies [45]. An increase of the photon-beam asymmetry with beam energy is more clearly illustrated.

Assuming t-channel dominance, based on the observed forward-peaking feature in the differential cross sections, positive values of the photon-beam asymmetry suggest a dominance of natural-parity exchange of K^* compared with the unnatural-parity exchange of K in the t-channel toward large E_γ. Large photon-beam asymmetries are also observed at $E_\gamma = 16$ GeV by SLAC [6]. Furthermore the photon-beam asymmetries for $K^+\Sigma^0$ production are slightly larger than those for

$K^+\Lambda$ production at $E_\gamma > 2.4$ GeV. This indicates a relatively weaker strength of unnatural-parity K-exchange in $K^+\Sigma^0$ production. These interpretations are consistent with what we observe in the t-dependence of the differential cross sections in Sec. III A.

For the photon-beam asymmetry of $K^+\Lambda$ production below $E_\gamma = 2.1$ GeV and $K^+\Sigma^0$ production below $E_\gamma = 2.4$ GeV in Fig. 6, the inclusion of contributions from nucleon resonances in the s-channel is crucial, judging from differences between data and the predictions from Regge trajectories only (RPR-Regge). This feature is also found in a comparison of the production cross sections. For $K^+\Lambda$ production above $E_\gamma = 2.1$ GeV, all predictions from RPR, RPR-Regge and BG converge at $\cos\theta^{K^+}_{c.m.} > 0.75$ and show certain deviations from the data. This suggests the need of including additional resonance contributions or a re-determination of Regge contributions with the current new data at forward angels.

For $K^+\Sigma^0$ production, the RPR model with no significant nucleon contributions overestimates the photon-beam asymmetries at $E_\gamma > 2.3$ GeV for all three angular bins, while the BG model gives a very good description of the photon-beam asymmetries over the whole region. It is noted that nucleon resonances with spin J larger than $3/2$ are not included in the RPR model [36] but they are taken into account in the BG model [33–35]. This difference of including higher-spin resonances might account for the better prediction of photon-beam asymmetries in the BG model.

In Fig. 8, the photon-beam asymmetry results for $K^+\Lambda$ and $K^+\Sigma^0$ as a function of $\cos\theta^{K^+}_{c.m.}$ are shown in six E_γ bins together with the previous results from LEPS [10] and the theoretical predictions. The agreement with previous measurements is reasonably good. Across all energy bins of E_γ from 1.8 to 3.0 GeV, the photon-beam asymmetries for the $K^+\Sigma^0$ channel at the forward angles of $0.6 < \cos\theta^{K^+}_{c.m.} < 1.0$ show a decrease toward zero. Such a decrease could reflect an increasing contribution of unnatural-parity K-exchange at smaller production angles, besides the trivial kinematic effect of a vanishing photon-beam asymmetry at zero degrees. For $E_\gamma \leq 2.3$ GeV, both RPR and BG models describe the data well and the BG model clearly does a better job in describing the photon-beam asymmetries of $K^+\Sigma^0$ channels for $E_\gamma > 2.3$ GeV.

IV. SUMMARY

In summary, we performed a measurement of differential cross sections and photon-beam asymmetries for the reactions $\gamma p \to K^+\Lambda$ and $K^+\Sigma^0$. The measured photon energy range of the results is 1.5-3.0 GeV, with a very forward angular coverage of $0.6 < \cos\theta^{K^+}_{c.m.} < 1.0$. The data

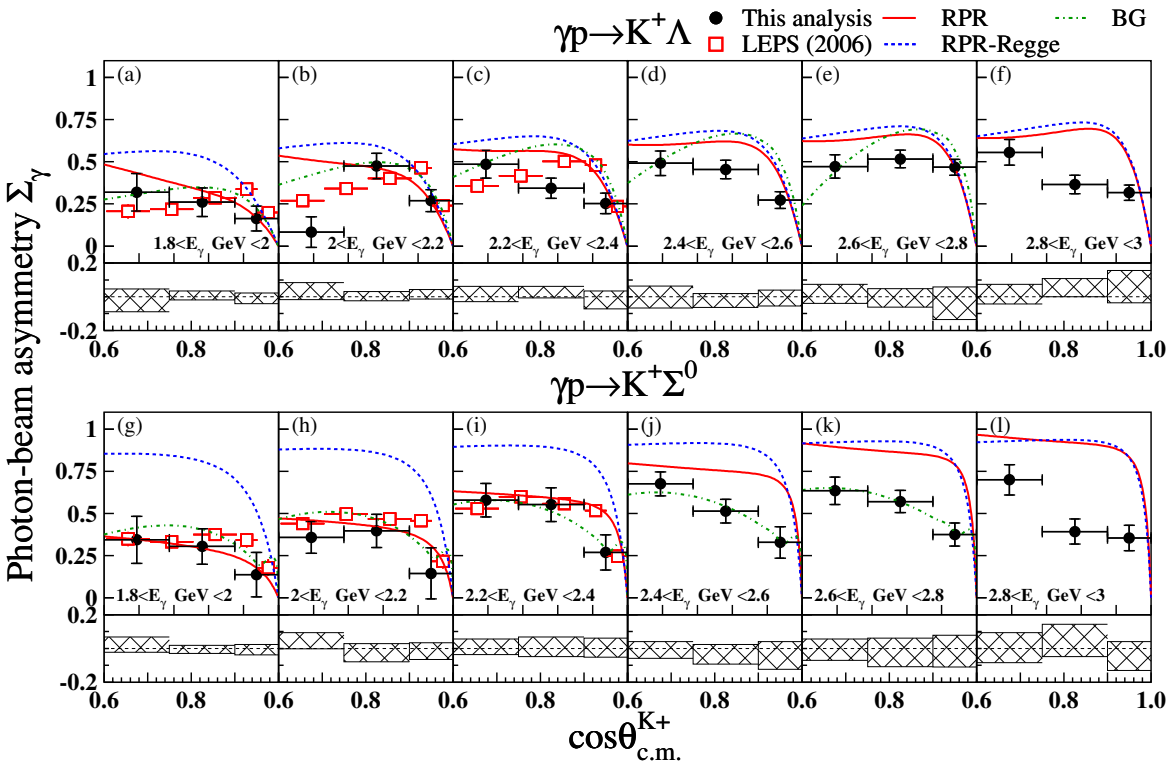

FIG. 8. Photon-beam asymmetries (Σ_γ) for the $p(\gamma,K^+)\Lambda$ reaction (a)$\sim$(f) and $p(\gamma,K^+)\Sigma^0$ reaction (g)$\sim$(l) with systematic uncertainty plotted in hatched histogram as a function of $\cos\theta^{K^+}_{c.m.}$ for $1.8 < E_\gamma < 3.0$ GeV. The results of this measurement and, LEPS 2006 are shown by solid black circles and red open squares. The notations of curves are the same as those in Fig. 3.

are in good agreement with results from previous measurements [10].

The production cross sections decrease slowly with increasing photon beam energy E_γ. There is no observation of distinct narrow structures in the energy dependence of either reaction. For $K^+\Lambda$ production, there is a clear forward-peaking feature in the angular distributions toward large E_γ, consistent with t-channel dominance for diffractive production at higher energies. The $K^+\Sigma^0$ channel shows less energy and angular dependence, compared to $K^+\Lambda$. This might reflect that s-channel contributions from nucleon resonances are more effective in the production of $K^+\Sigma^0$. Based on the reggeized t-channel framework, the results of cross sections near $t = t_{min}$ provide evidence of the existence of K-exchange in $K^+\Lambda$ production at low energies.

The photon-beam asymmetries for both $K^+\Lambda$ and $K^+\Sigma^0$ channels are all positive. This suggests a dominating natural-parity exchange of K^* in the t-channel. At $E_\gamma > 2.4$ GeV, the results deviate from the predictions of the t-channel Regge trajectories only. The BG model includ-

ing higher-spin nucleon resonances describes nicely the photon-beam asymmetries for the $K^+\Sigma^0$ channel up to $E_\gamma = 2.8$ GeV. All these observations strongly suggest the existence of nucleon resonance contributions at $E_\gamma = 2.4 - 3.0$ GeV.

A comparison with theoretical predictions from both RPR and BG models indicates that there is room for improvement of the theoretical modeling of Regge trajectories in t-channel as well as the contributions from the nucleon resonances. With the constraints of these new data of hyperon Λ and Σ^0 photoproduction at very forward angles for few-GeV photons, we look forward to the progress in theoretical modeling shortly.

ACKNOWLEDGMENTS

The authors gratefully acknowledge the contributions of the SPring-8 staff for supporting BL33LEP beamline and the LEPS experiment. The experiments were performed at the BL33LEP of SPring-8 with the approval of the Japan Synchrotron Radiation Research Institute (JASRI) as a contract beamline (Proposal No. BL33LEP/6001). We thank Terry Mart, Jan Ryckebusch, Sang-Ho Kim and Atsushi Hosaka for fruitful discussions. This work was supported in part by the Ministry of Science and Technology of Taiwan, the Ministry of Education, Science, Sports and Culture of Japan, the National Research Foundation of Korea. and the U.S. National Science Foundation,

---

[1] T. Mart, Int. J. Mod. Phys. E **19**, 2343 (2010).

[2] E. Klempt, A. V. Sarantsev and U. Thoma, EPJ Web Conf. **134**, 02002 (2017).

[3] R. G. Edwards, J. J. Dudek, D. G. Richards and S. J. Wallace, Phys. Rev. D **84**, 074508 (2011).

[4] V. Crede and W. Roberts, Rept. Prog. Phys. **76**, 076301 (2013).

[5] A. Boyarski *et al.*, Phys. Rev. Lett. **22**, 1131 (1969).

[6] D. J. Quinn, J. P. Rutherfoord, M. A. Shupe, D. J. Sherden, R. H. Siemann and C. K. Sinclair, Phys. Rev. D **20**, 1553 (1979).

[7] M. Q. Tran *et al.* (SAPHIR Collaboration), Phys. Lett. B **445**, 20 (1998).

[8] K.-H. Glander *et al.* (SAPHIR Collaboration), Eur. Phys. Jour. A **19**, 251 (2004).

[9] R. G. T. Zegers *et al.* (LEPS Collaboration), Phys. Rev. Lett. **91**, 092001 (2003).

[10] M. Sumihama *et al.* (LEPS Collaboration), Phys. Rev. C **73**, 035214 (2006).

[11] K. Hicks *et al.* (LEPS Collaboration), Phys. Rev. C **76**, 042201(R) (2007).

[12] R. Bradford *et al.* (CLAS Collaboration), Phys. Rev. C **73**, 035202 (2006).

[13] M. E. McCracken *et al.* (CLAS Collaboration), Phys. Rev. C **81**, 025201 (2010).

[14] B. Dey *et al.* (CLAS Collaboration), Phys. Rev. C **82**, 025202 (2010).

[15] A. Lleres *et al.* (GRAAL Collaboration), Eur. Phys. J. A **31**, 79 (2007).

[16] A. Lleres *et al.* (GRAAL Collaboration), Eur. Phys. J. A **39**, 149 (2009).

[17] T. C. Jude *et al.* (Crystal Ball Collaboration), Phys. Lett. B **735**, 112 (2014).

[18] H. Kohri *et al.* (LEPS Collaboration), Phys. Rev. Lett. **97**, 082003 (2006).

[19] S. A. Pereira *et al.* (CLAS Collaboration), Phys. Lett. B **688**, 289 (2010).

[20] S. Goers *et al.* (SAPHIR Collaboration), Phys. Lett. B **464**, 331 (1999).

[21] R. Lawall *et al.* (SAPHIR Collaboration), Eur. Phys. J. A **24**, 275 (2005).

[22] R. Castelijns *et al.* (CBELSA/TAPS Collaboration), Eur. Phys. J. A **35**, 39 (2008).

[23] R. Ewald *et al.* (CBELSA/TAPS Collaboration), Phys. Lett. B **713**, 180 (2012).

[24] P. Aguar-Bartolome *et al.* (A2 Collaboration), Phys. Rev. C **88**, 044601 (2013).

[25] T. Mart and C. Bennhold, Phys. Rev. C **61**, 012201(R) (1999).

[26] T. Mart, Phys. Rev. C **90**, 065202 (2014).

[27] T. Mart, S. Clymton and A. J. Arifi, Phys. Rev. D **92**, 094019 (2015).

[28] T. Mart and S. Sakinah, Phys. Rev. C **95**, 045205 (2017).

[29] M. Guidal, J. M. Laget and M. Vanderhaeghen, Nucl. Phys. A **627**, 645 (1997).

[30] M. Guidal, J. M. Laget and M. Vanderhaeghen, Phys. Rev. C **68**, 058201 (2003).

[31] A. V. Sarantsev, V. A. Nikonov, A. V. Anisovich, E. Klempt and U. Thoma, Eur. Phys. J. A **25**, 441 (2005).

[32] A. V. Anisovich, V. Kleber, E. Klempt, V. A. Nikonov, A. V. Sarantsev and U. Thoma, Eur. Phys. J. A **34**, 243 (2007).

[33] A. V. Anisovich, E. Klempt, V. A. Nikonov, A. V. Sarantsev and U. Thoma, Eur. Phys. J. A **47**, 27 (2011).

[34] A. V. Anisovich, E. Klempt, V. A. Nikonov, A. V. Sarantsev and U. Thoma, Eur. Phys. J. A **47**, 153 (2011).

[35] E. Gutz *et al.* (CBELSA/TAPS Collaboration), Eur. Phys. J. A **50**, 74 (2014).

[36] T. Corthals, J. Ryckebusch, and T. Van Cauteren, Phys. Rev. C **73**, 045207 (2006).

[37] T. Corthals, T. Van Cauteren, J. Ryckebusch, and D. G. Ireland, Phys. Rev. C **75**, 045204 (2007).

[38] L. De Cruz, J. Ryckebusch, T. Vrancx, and P. Vancraeyveld, Phys. Rev. C **86**, 015212 (2012).

[39] A. V. Anisovich *et al.*, Phys. Rev. Lett. **119**, 062004 (2017).

[40] N. Muramatsu *et al.*, Nucl. Instrum. Methods A **737**, 184 (2014).

[41] S. H. Hwang *et al.* (LEPS Collaboration), Phys. Rev. Lett. **108**, 092001 (2012).

[42] T. Nakano *et al.* (LEPS Collaboration), Nucl. Phys. A **684**, 71 (2001).

[43] `http://rprmodel.ugent.be/calc/`

[44] `http://pwa.hiskp.uni-bonn.de/BG2014_02_obs_int.htm`

[45] M. Sumihama, Ph.D. thesis, Osaka University, 2003.